

Unexpected enhancement of ferroelectricity in HfO₂ on SiO₂ and GeO₂

Shihui Zhao¹⁺, Bowen Li²⁺, Huanglong Li^{*2,3}

¹ School of Materials Science and Engineering, Tsinghua University, Beijing, 100084, China ² Department of Precision Instrument, Center for Brain Inspired Computing Research, Tsinghua University, Beijing, 100084, China ³ Chinese Institute for Brain Research, Beijing, 102206, China

⁺equal contributions

*Email: li_huanglong@mail.tsinghua.edu.cn

Abstract

Ferroelectric HfO₂ (fe-HfO₂) has garnered increasing research interest for nonvolatile memories and low-power transistors. However, many challenges are to be resolved. One of them is the depolarizing effect that is commonly attributed to the formation of fe-HfO₂: electrode interface. In addition to this interface, it is not hard to find that HfO₂ is rarely used in isolation but most often in combination with non-ferroelectric dielectric in real device for practical reasons. This leads to the formation of fe-HfO₂: dielectric interface. Recently, counterintuitive enhancement of ferroelectricity in fe-HfO₂ grown on SiO₂ has been discovered experimentally, opening up a previously unknown region in design space. Yet, a deeper understanding of the role of SiO₂ in enabling the enhanced ferroelectricity in fe-HfO₂ still lacks. Here, we investigate the electronic structures of ten fe-HfO₂: oxide dielectric interfaces. We find that while in most cases, as expected, interface formation introduces depolarizing fields in fe-HfO₂, SiO₂ and GeO₂ stand out as two abnormal dielectrics in the sense that they surprisingly hyperpolarize fe-HfO₂, in consistence with the experimental findings. We provide explanations from a chemical bonding perspective. This work suggests that the interplay between fe-HfO₂ and non-ferroelectric dielectric is nontrivial and cannot be neglected toward an improved understanding of HfO₂ ferroelectricity.

Introduction

The replacement of SiO₂ with high-K HfO₂ in the transistor device¹ has been considered as one of the biggest redesign of the transistor technology, enabling continued down-scaling of the transistor according to the prediction of Moore's law. Even though successfully introduced into microelectronics, the function of HfO₂ has traditionally been viewed to be no more than electrical insulation.

Today, aggressive transistor scaling down to 3nm is on the way² at which the semiconductor community is becoming increasingly concerned about the ending of Moore's law. To tackle this challenge, the industry roadmap has laid out development plan that is not centred on Moore's law.³ Instead, it now calls for functionality-driven development, known as the More than Moore strategy. The More than Moore approach welcomes emerging devices that incorporate functionalities that do not necessarily scale according to Moore's Law, but provides additional value in different ways.⁴

While the workings of the transistor are purely electronic, there are a plethora of functional materials that can provide ionic degree of freedom. Ferroelectricity is a well-known but rare materials property that is produced by spontaneous ion displacement. This requires the crystal to have non-centrosymmetric structure. Historically, this materials requirement could only be satisfied in complex crystals, such as perovskites, which are unfortunately not CMOS-compatible.^{5, 6} In 2011, a group of German researchers reported an unexpected discovery of ferroelectricity in Si-doped crystalline HfO₂.^{7, 8} Because HfO₂ had already been a key enabler of the high-K-metal-gate technology for transistors since 2007, this discovery has led to a re-emergence of intensive research interest in ferroelectric devices.

Ferroelectric device is a very promising device concept in addressing the power consumption issue that arises from the subthreshold leakage with continued transistor scaling. In the past decade, the negative-capacitance transistor has been extensively studied as an emerging low-power solution.⁹⁻¹² This transistor exploits the inherent instability of ferroelectric gate oxide in field-driven ferroelectric transition. Low-subthreshold-leakage transistors based on ferroelectric HfO₂ (fe-HfO₂) have been demonstrated.¹³⁻¹⁷ To provide sufficient capacitance matching and maintain the overall gate capacitance positive, the transistor uses series ferroelectric: dielectric gate capacitor instead of a single ferroelectric one.

In addition to the scaling issues, the problem of the increasing logic-memory speed gap in conventional von Neumann computing architecture¹⁸ in which a memory hierarchy is formed by devices with varying speeds has also been exacerbated with the rise of data-abundant computing and compute-extensive artificial intelligence applications. DRAM as the primary memory has high speed but its memory is volatile that power is required to maintain the stored information. Therefore, emerging memory devices with both nonvolatile data storage and potentially high speed have been actively pursued as the replacements of incumbent memories.¹⁹ Among them, ferroelectric transistor memory is very promising.^{5, 6} It adopts a

ferroelectric gate oxide and uses ferroelectric polarization for data storage. In practice, a ferroelectric: dielectric double-layer is used for improved quality of the gate stack: semiconductor interface.²⁰ In addition to three-terminal devices, two-terminal ferroelectric tunneling junction (FTJ) memories based on resistive readout have also been considered as strong contenders for using in mainstream computer systems and replacing their commercially available predecessors based on capacitive readout in various system-on-chip applications.²¹⁻²³

More radical solutions to the von Neumann bottleneck include in-memory computing and neuromorphic computing where individual nonvolatile memory device plays the roles of both memory and computation.²⁴ fe-HfO₂-based ferroelectric transistor and FTJ computational memories have demonstrated tantalizing potential.²⁵⁻²⁹ Many of these prototype devices adopted a ferroelectric: dielectric double-layer structure, in particular, fe-HfO₂: SiO₂.

Although fe-HfO₂-based devices have been considered as important “More than Moore” technologies, their developments have faced many challenges. One of them is the depolarizing effect that is commonly attributed to the formation of fe-HfO₂: electrode interface with insufficient screening of the bound charge on the fe-HfO₂ side.^{30,31} Generally, the depolarizing effects are stronger in thinner fe-HfO₂ films that are desired for optimal efficiency and information storage density. This reduces the dielectric responses and causes rapid polarization relaxations.³¹ In addition to the fe-HfO₂: electrode interfaces, it is not hard to find from the above introduction that HfO₂ is rarely used in isolation but most often in combination with non-ferroelectric dielectric in real device for practical reasons. Despite the ubiquity of the ferroelectric: dielectric double-layer structure in the emerging fe-HfO₂-based devices, the studies on their interface properties are still rare. Unlike the conventional non-ferroelectric HfO₂: dielectric interfaces that have been extensively investigated,³²⁻³⁵ fe-HfO₂: dielectric interfaces are places where electronic charge degree of freedom is strongly coupled to ionic lattice degree of freedom, possibly giving rise to many emergent phenomena, such as the formation of two-dimensionally confined electron gas (2DEG).³⁶⁻⁴¹

Recently, Cheema et al.⁴² reported counterintuitive enhancement of ferroelectricity in ultrathin HfO₂ film grown on SiO₂, opening up previously unknown region in design space and offering unexpected opportunities for fe-HfO₂-based technologies. However, a deeper understanding of the role of SiO₂ in enabling the enhanced ferroelectricity in fe-HfO₂ still lacks. In this work, we investigate several representative fe-HfO₂: oxide dielectric interfaces by first-principles calculations. The oxide dielectrics under consideration cover a range of cation valence, electronegativity and band gaps. Anomalies are found in fe-HfO₂: SiO₂ and fe-HfO₂: GeO₂ interface systems.

Results and discussion

We create supercell models of several fe-HfO₂: oxide dielectric interfaces, including fe-HfO₂: Al₂O₃, fe-HfO₂: La₂O₃, fe-HfO₂: SiO₂ (quartz), fe-HfO₂: GeO₂, fe-HfO₂: m-HfO₂ (m for

monoclinic), fe-HfO₂: t-HfO₂ (t for tetragonal), fe-HfO₂: TiO₂, fe-HfO₂: P₂O₅, fe-HfO₂: Ta₂O₅ and fe-HfO₂: WO₃, each containing roughly 25 Å thick fe-HfO₂ and oxide dielectric with comparable thickness. The fe-HfO₂ model is selected to be the polar orthorhombic Pca₂₁ phase which has generally been considered as the source of ferroelectricity,^{43, 44} while other ferroelectric phases have also been proposed.^{45, 46} In this fe-HfO₂ model, the displacements of the three-fold oxygen ions (O_{III}²⁻) along the c axis give rise to ferroelectric polarizations. The electron-counting-rule is satisfied in each model. The in-plane lattice constants are fixed to the ones calculated for fe-HfO₂ single crystal, and the lattice perpendicular to the interface is relaxed, using the CASTEP code.⁴⁷ The calculations use the generalized gradient approximation (GGA)⁴⁸ and ultrasoft pseudopotentials with a plane wave cutoff energy of 380 eV.

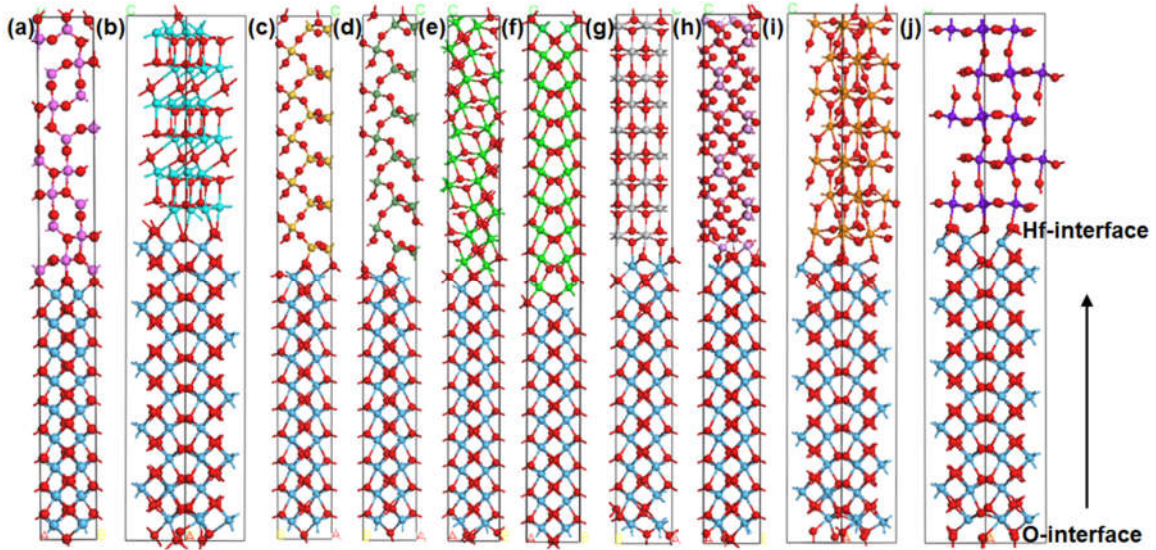


Figure 1 Atomic structures of the (a) fe-HfO₂: Al₂O₃, (b) fe-HfO₂: La₂O₃, (c) fe-HfO₂: SiO₂, (d) fe-HfO₂: GeO₂, (e) fe-HfO₂: m-HfO₂, (f) fe-HfO₂: t-HfO₂, (g) fe-HfO₂: TiO₂, (h) fe-HfO₂: P₂O₅, (i) fe-HfO₂: Ta₂O₅ and (j) fe-HfO₂: WO₃ interface systems, respectively. The arrow shows the direction of ferroelectric polarization.

In all interface models, the polarizations of fe-HfO₂ are sustained after geometry optimizations, as seen in figure 1(a-j). All these models are shown with the polarizations of fe-HfO₂ in the upward directions. The two asymmetric interfaces in each model with Hf⁴⁺ bound charge and O_{III}²⁻ bound charge are referred to as the Hf-interface and O-interface, respectively. The projected density of states (PDOS) of each model is shown in figure 2(a-j). For fe-HfO₂: m-HfO₂, the bands of fe-HfO₂ bend toward higher energy as they approach the O-interface. Similarly, the bands of m-HfO₂ also bend toward higher energy as they approach the O-interface. These result in wedge-shaped potential wells for electrons and holes at the Hf-interface and O-interface, respectively. The Fermi energy (E_f) of this interface system lies close to the conduction band minimums (CBMs) of fe-HfO₂ and m-HfO₂ at the Hf-interface, and lies

close to their valence band maximums (VBMs) at the O-interface. As the thickness of fe-HfO₂ increases, the E_f is expected to intersect the band edges at the two interfaces, giving rise to 2DEG and two-dimensionally confined hole gas (2DHG), respectively. Experimentally, 2DEG has indeed been observed at the perovskite ferroelectric: dielectric interface system.³⁶

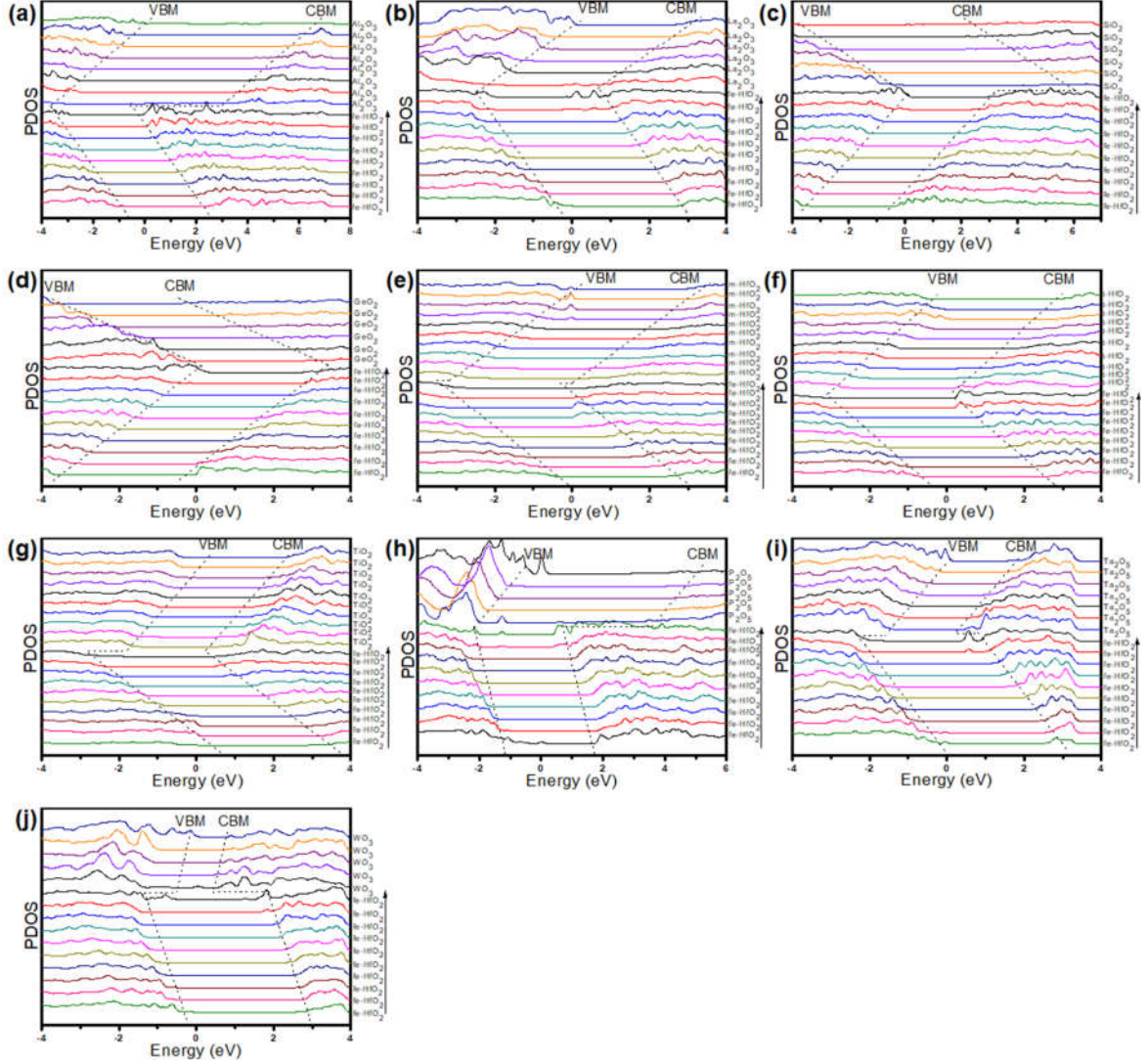


Figure 2 PDOSs of the (a) fe-HfO₂: Al₂O₃, (b) fe-HfO₂: La₂O₃, (c) fe-HfO₂: SiO₂, (d) fe-HfO₂: GeO₂, (e) fe-HfO₂: m-HfO₂, (f) fe-HfO₂: t-HfO₂, (g) fe-HfO₂: TiO₂, (h) fe-HfO₂: P₂O₅, (i) fe-HfO₂: Ta₂O₅ and (j) fe-HfO₂: WO₃ interface systems, respectively. The Fermi energies are set to 0 eV.

The direction of band bending in fe-HfO₂ indicates the existence of a depolarizing field that tends to destabilize its ferroelectric polarization, posing challenges to the reliability of ferroelectric devices. The existence of this depolarizing field is explainable under the tenet of macroscopic electrostatic theory^{49, 50}. Normally, the depolarizing field in a ferroelectric in the

formation of ferroelectric: metallic electrode interface is weaker if the metallic electrode is of shorter Thomas-Fermi screening length^{22, 30} or with certain degree of ionic relaxation.⁵¹ The tendency to form 2DEG (2DHG) at the Hf-interface (O-interface) in ferroelectric: dielectric stack can be viewed as another possible source to screen the depolarizing field.³⁷

The fe-HfO₂: t-HfO₂ interface system shows similar band structure properties to those of the fe-HfO₂: m-HfO₂ system. The dynamic structural transitions between fe-HfO₂ and m-HfO₂, and between fe-HfO₂ and t-HfO₂ have been considered to be vital in understanding the field-cycling behavior of fe-HfO₂-based ferroelectric capacitors.^{42, 53} The depolarizing field as a result of the formation of fe-HfO₂: m-HfO₂ and fe-HfO₂: t-HfO₂ grain boundaries may further decrease the cycling lifetime of fe-HfO₂.

For interfaces between fe-HfO₂ and other metal-oxide dielectrics, namely, Al₂O₃, La₂O₃, TiO₂, Ta₂O₅ and WO₃, similar interfacial band structure properties to those of fe-HfO₂: m-HfO₂ and fe-HfO₂: t-HfO₂ interfaces are found, in consistence with the recent theoretical findings.⁵⁴ As previously introduced, the ferroelectric: dielectric double-layer structure is critical in NC transistors and ferroelectric transistors. In the formation of ferroelectric: dielectric interface, the density of the induced screening bound charge on the dielectric side, according to the macroscopic electrostatic theory, is so high that the dielectric would have already been broken down. To resolve this discrepancy, it has been proposed that the total required screening charge is balanced by the leakage charge trapped at the interface²⁰. Alternatively, our results show that the formation of 2DEG (2DHG) at the Hf-interface (O-interface) could also be a source of the screening charge.

Anomalies, however, are found in fe-HfO₂: SiO₂ and fe-HfO₂: GeO₂ interface systems. As seen from its PDOS (fig. 2(c, d)), fe-HfO₂ bands bend toward lower energy as they approach the O-interface; at the same time, SiO₂ bands also bend toward lower energy as they approach the O-interface. These trends of band bending are in contrast to those found in other fe-HfO₂: oxide systems, resulting in the possibility of forming 2DEG (2DHG) at the O (Hf)-interface, rather than at the Hf (O)-interface. Band bending in fe-HfO₂ in such a way indicates that the field inside fe-HfO₂ does not tend to reduce the ferroelectric polarization, but instead enhances it. At the first sight, this is counterintuitive.

In addition to macroscopic electrostatics, microscopic-level interfacial atomic interactions have also been believed to affect ferroelectricity. Duan et al.⁵⁵ reported enhanced ferroelectricity in fe-KNbO₃: Pt interface system compared to that in bulk fe-KNbO₃. This was attributed to the weak interfacial interactions that allow the interfacial ions on the fe-KNbO₃ side to be easily displaced in-line with the ferroelectric polarization. Similarly, Stengel et al.⁵⁶ reported anomalous enhancement of the ferroelectricity resulting from oxygen-metal bond mechanisms at the ferroelectric: metal electrode interface in which the metal is very inert, such as Pt and Au, and thus the oxygen-metal bonds are quite unstable. As a result, interfacial polarizations are formed as continuations of the ferroelectric polarization. In Stengel's case, hyperpolarizing field, rather than depolarizing field, was built up in the ferroelectric; in other words, the bound

charge on the ferroelectric side was over-screened. Similar interfacial polarization effects in systems where ferroelectrics are grown on conductive metal-oxide electrode SrRuO_3 ⁴¹ or insulating SrTiO_3 ⁵⁷ have also been proposed to account for the enhancement of screening.

Figure 3 compares the ionic displacements in various oxide dielectrics near the interfaces and in their interiors. The separation between the center of three layers of O anions and the center of two layers of cations that are closest to the interface is calculated, characterizing the strength of interfacial polarization. The coordinates of the third interfacial layer of O anions and the more interior ions are used to calculate the interior polarization. It is noted that for all oxides the interfacial polarizations near the Hf-interfaces are in-line with the polarizations of fe-HfO₂. Under the tenet of macroscopic electrostatic theory, such interfacial polarization as a continuation of fe-HfO₂ polarization, if strong enough, may induce overscreening effect that the total bound charge at the Hf-interface is effectively negative and therefore the field in fe-HfO₂ may be hyperpolarizing. Among these oxides, however, only SiO₂ and GeO₂ hyperpolarize fe-HfO₂. This can be understood from the strong interfacial polarization (overscreening) near the Hf-interface. For GeO₂, although the interfacial polarization near the O-interface tends to depolarize fe-HfO₂, it is weak enough that it does not compromise the hyperpolarizing effect induced at the Hf-interface. Other oxides do not hyperpolarize fe-HfO₂ because of the relatively weak screening effects (Al_2O_3 , m-HfO₂, t-HfO₂, TiO₂, Ta₂O₅, P₂O₅ and WO₃) at the Hf-interfaces or (and) the strong depolarizing effects at the O-interfaces (La_2O_3 , P₂O₅ and WO₃). It is also seen that the directions of the interior polarizations of all oxide dielectrics, except for SiO₂ and GeO₂, are the same as that of fe-HfO₂ polarization. These can be easily understood as the results of ionic displacements in response to the built-in electric field.

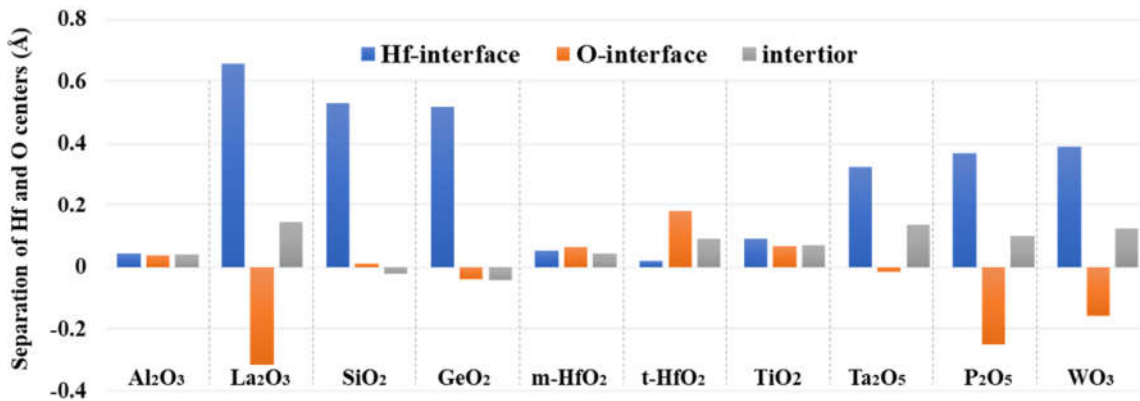


Figure 3 Ionic displacements for various fe-HfO₂: oxide systems near the interfaces and in the interiors of the oxides. Positive values indicate that polarizations are in the same direction as those of HfO₂ ferroelectric polarizations.

The overall hyperpolarizing effects on fe-HfO₂ in the fe-HfO₂: SiO₂ and fe-HfO₂: GeO₂ systems are similar to that observed in the fe-BaTiO₃: Pt system⁵⁶ where Pt-O interfacial

polarizations as continuations of the fe-BaTiO₃ polarization take place at the two asymmetric interfaces. Microscopically, this has been linked to the weak or unstable Pt-O bond that there is no strong enough restoring force associated with it against ferroelectric polar distortion. The stabilities of the interfacial M-O (M: Al, La, Si, Ge, Ti, Hf, Ta, P, W) bonds are analyzed by calculating the crystal orbital Hamilton populations (COHP),⁵⁸ as shown in figure 4. It is seen that interfacial La-O, Si-O, Ge-O and P-O bonds are relatively unstable with relatively strong antibonding characteristics below their respective E_f, in contrast to other types of interfacial bonds. These interfacial bond instabilities coincide with their strong interfacial polarizations at the Hf-interfaces as continuations of fe-HfO₂ polarizations, as shown in figure 3.

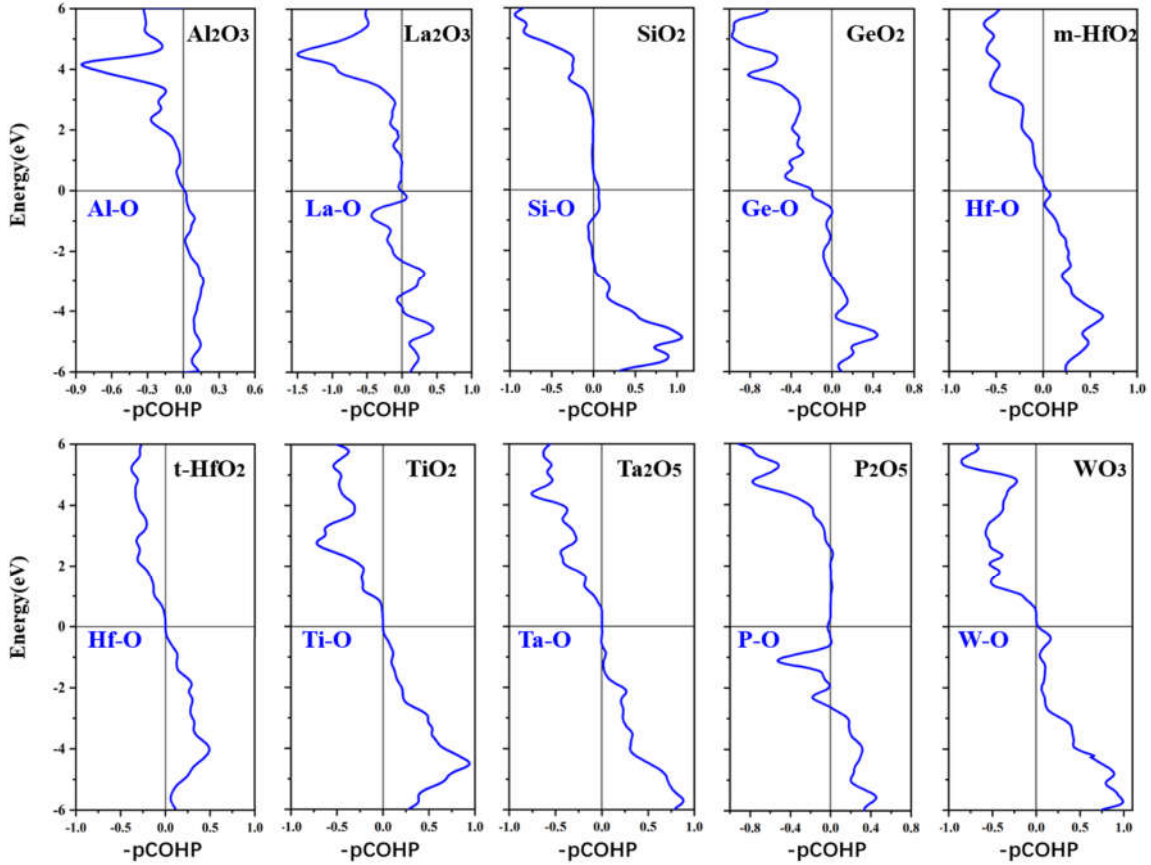


Figure 4 Crystal Orbital Hamilton Population (COHP) analysis for the interfacial M-O (M: Al, La, Si, Ge, Hf, Ti, Ta, P, W) bonds. Positive (negative) pCOHP values indicate bonding (antibonding) characteristics. Horizontal lines denote the Fermi levels.

The overall strong interfacial polarization as the continuation of fe-HfO₂ polarization in the fe-HfO₂: SiO₂ system (fe-HfO₂: GeO₂ is similar) requires the interfacial O→Si bond and (or) Si→O bond at the Hf-interface and O-interface, respectively, to be longer and shorter than normal (→points in the fe-HfO₂ polarization direction), in analogy to the nonequivalent interfacial Pt-O bond configurations in the non-centrosymmetric Pt-ferroelectric-Pt structure

with enhanced ferroelectricity.⁵⁶ SiO₂ has the ability to form such long and short bonds, as can be understood from the intrinsic nonequivalency of the Si-O bonds in bulk SiO₂ (GeO₂ is similar). Bulk quartz SiO₂ is a three-dimensionally connected network with alternating short and long Si-O bonds.⁵⁹ The short and long bonds are switchable by cooperative atom displacements, giving rise to double-well potential landscape.⁶⁰ Compared to SiO₂ and GeO₂, however, P₂O₅ has less connected network (more molecular) within which cooperative atom displacements are less effective, and La₂O₃ has more asymmetric adiabatic potential-energy surface that bond compression is not as easy as bond stretching.⁶¹ Therefore, although fe-HfO₂: P₂O₅ and fe-HfO₂: La₂O₃ systems show strong interfacial polarizations as the continuations of fe-HfO₂ polarizations at their respective Hf-interfaces, the less effectiveness in inducing polarizations of the same directions at the O-interfaces eventually reduces the overall screening effects.

Conclusion

To conclude, by investigating ten fe-HfO₂: oxide interface systems, we observe anomalies in fe-HfO₂: SiO₂ and fe-HfO₂: GeO₂ systems that induce hyperpolarizing fields in fe-HfO₂. The SiO₂ and GeO₂ anomalies can be understood from the interfacial bond instabilities and, indispensably, their bulk covalent bond properties. The enhanced ferroelectricity in ultrathin HfO₂ film on a SiO₂ has previously been explained as due to strain effect.⁴² Although strain effect^{55, 62-64} has frequently been invoked to explain ferroelectric anomalies, our results suggest that a more chemical interpretation is also likely. Our work advances the understanding of ferroelectric/dielectric stacks and suggests that the interplay between ferroelectric HfO₂ and non-ferroelectric oxide dielectric is nontrivial and cannot be neglected toward an improved understanding of HfO₂ ferroelectricity.

Notes

The authors declare no competing financial interest.

Acknowledgments

The authors acknowledge funding from National Natural Science Foundation (grant no. 61974082, 61704096 and 61836004). The authors acknowledge funding from National Key R&D Program of China (2018YFE0200200), Youth Elite Scientist Sponsorship (YESS) Program of China Association for Science and Technology (CAST) (no. 2019QNRC001), supercomputing wales project number scw1070, Tsinghua-IDG/McGovern Brain-X program, Beijing science and technology program (grant no. Z181100001518006 and

Z191100007519009), the Suzhou-Tsinghua innovation leading program 2016SZ0102, and CETC Haikang Group-Brain Inspired Computing Joint Research Center.

References

1. Mistry K, Allen C, Auth C, et al. A 45nm Logic Technology with High-k+Metal Gate Transistors, Strained Silicon, 9 Cu Interconnect Layers, 193nm Dry Patterning, and 100% Pb-free Packaging. In: *2007 IEEE International Electron Devices Meeting (IEDM)*. 2007:247-250.
2. Ye P, Ernst T, Khare MV. The last silicon transistor: Nanosheet devices could be the final evolutionary step for Moore's Law. *IEEE Spectr*. 2019;56:30-35.
3. Waldrop MM. The chips are down for Moore's law. *Nature*. 2016;530:144-7.
4. Arden W, Brillouët M, Coge P, Graef M, Huizing B, Mahnkopf R. "More-than-Moore" White Paper. *The International Technology Roadmap for Semiconductors (ITRS)*. 2010.
5. Khan AI, Keshavarzi A, Datta S. The future of ferroelectric field-effect transistor technology. *Nat Electron*. 2020;3:588-597.
6. Mikolajick T, Slesazek S, Mulaosmanovic H, et al. Next generation ferroelectric materials for semiconductor process integration and their applications. *J Appl Phys*. 2021;129:100901.
7. Böске TS, Müller J, Bräuhaus D, Schröder U, Böttger U. Ferroelectricity in hafnium oxide: CMOS compatible ferroelectric field effect transistors. In: *2011 International Electron Devices Meeting (IEDM)*. 2011:24.5.1-24.5.4.
8. Böске TS, Teichert S, Bräuhaus D, et al. Phase transitions in ferroelectric silicon doped hafnium oxide. *Appl Phys Lett*. 2011;99:112904.
9. Salahuddin S, Datta S. Use of negative capacitance to provide voltage amplification for low power nanoscale devices. *Nano Lett*. 2008;8:405.
10. Alam MA, Si M, Ye PD. A critical review of recent progress on negative capacitance field-effect transistors. *Appl Phys Lett*. 2019;114:090401.
11. Hoffmann M, Slesazek S, Schroeder U, Mikolajick T. What's next for negative capacitance electronics? *Nat Electron*. 2020;3:1-3.
12. Íñiguez J, Zubko P, Luk'yanchuk I, Cano A. Ferroelectric negative capacitance. *Nat Rev Mater*. 2019;4:243-256.
13. Cheng CH, Chin A. Low-Voltage Steep Turn-On pMOSFET Using Ferroelectric High- κ Gate Dielectric. *IEEE Electron Device Lett*. 2014;35:274-276.
14. Lee MH, Chen PG, Liu C, et al. Prospects for ferroelectric HfZrOx FETs with experimentally CET=0.98nm, SSfor=42mV/dec, SSrev=28mV/dec, switch-off $\leq 0.2V$, and hysteresis-free strategies. In: *2015 IEEE International Electron Devices Meeting (IEDM)*. 2015:22.5.1-22.5.4.
15. Li KS, Chen PG, Lai TY, et al. Sub-60mV-swing negative-capacitance FinFET without hysteresis. In: *2015 IEEE International Electron Devices Meeting (IEDM)*. 2015:22.6.1-22.6.4.
16. Nourbakhsh A, Zubair A, Joglekar S, Dresselhaus M, Palacios T. Subthreshold swing improvement in MoS₂ transistors by the negative-capacitance effect in a ferroelectric Al-doped-HfO₂/HfO₂ gate dielectric stack. *Nanoscale*. 2017;9:6122-6127.

17. Si M, Su C-J, Jiang C, et al. Steep-slope hysteresis-free negative capacitance MoS₂ transistors. *Nat Nanotechnol.* 2018;13:24-28.
18. Sayeef S, Ni K, Suman D. The era of hyper-scaling in electronics. *Nat Electron.* 2018;1:442-450.
19. Chen A. A review of emerging non-volatile memory (NVM) technologies and applications. *Solid-State Electron.* 2016;125:25-38.
20. Si M, Xiao L, Ye PD. Ferroelectric Polarization Switching of Hafnium Zirconium Oxide in a Ferroelectric/Dielectric Stack. *ACS Appl Electron Mater.* 2019;1:745-751.
21. Chanthbouala A, Crassous A, Garcia V, et al. Solid-state memories based on ferroelectric tunnel junctions. *Nat Nanotechnol.* 2012;7:101-104.
22. Garcia V, Bibes M. Ferroelectric tunnel junctions for information storage and processing. *Nat Commun.* 2014;5:4289.
23. André C, Garcia V, Cherifi R, et al. A ferroelectric memristor. *Nat Mater.* 2012;11:860-4.
24. Daniele I, Philip HS. In-memory computing with resistive switching devices. *Nat Electron.* 2018;1:333-343.
25. Ni K, Yin X, Laguna AF, Joshi S, Datta S. Ferroelectric ternary content-addressable memory for one-shot learning. *Nat Electron.* 2019;2:521-529.
26. Myungsoo S, Kang MH, Seung-Bae J, et al. First Demonstration of a Logic-Process Compatible Junctionless Ferroelectric FinFET Synapse for Neuromorphic Applications. *IEEE Electron Device Lett.* 2018;39:1445-1448.
27. Jerry M, Chen P, Zhang J, et al. Ferroelectric FET analog synapse for acceleration of deep neural network training. In: *2017 IEEE International Electron Devices Meeting (IEDM).* 2017:6.2.1-6.2.4.
28. Dutta S, Schafer C, Gomez J, Ni K, Datta S. Supervised Learning in All FeFET-Based Spiking Neural Network: Opportunities and Challenges. *Front Neurosci.* 2020;14:634.
29. Berdan R, Marukame T, Ota K, et al. Low-power linear computation using nonlinear ferroelectric tunnel junction memristors. *Nat Electron.* 2020;3:1-8.
30. Junquera J, Ghosez P. Critical thickness for ferroelectricity in perovskite ultrathin films. *Nature.* 2003;422:506-509.
31. Dawber M, Rabe KM, Scott J F. Physics of thin-film ferroelectric oxides. *Rev Mod Phys.* 2005;77:1083-1130.
32. Kirsch PD, Sivasubramani P, Huang J, et al. Dipole model explaining high-k/metal gate field effect transistor threshold voltage tuning. *Appl Phys Lett.* 2008;92:615.
33. Kita K, Toriumi A. Origin of electric dipoles formed at high-k/SiO₂ interface. *Appl Phys Lett.* 2009;94:971.
34. Wang X, Han K, Wang W, et al. Physical origin of dipole formation at high-k/SiO₂ interface in metal-oxide-semiconductor device with high-k/metal gate structure. *Appl Phys Lett.* 2010;96:152907.
35. Lin L, Robertson J. Atomic mechanism of electric dipole formed at high-K: SiO₂ interface. *J Appl Phys.* 2011;109:327-2.
36. Zhang Y, Lu H, Xie L, et al. Anisotropic polarization-induced conductance at a ferroelectric-insulator interface. *Nat Nanotechnol.* 2018;13:1132-1136.
37. Niranjana MK, Wang Y, Jaswal SS, Tsymbal EY. Prediction of a Switchable Two-Dimensional Electron Gas at Ferroelectric Oxide Interfaces. *Phys Rev Lett.* 2009;103:016804.

38. Fredrickson KD, Demkov AA. Switchable conductivity at the ferroelectric interface: Nonpolar oxides. *Phys Rev B*. 2015;91:115126.
39. Zhen Z, Ping W, Lang C, Wang J. First-principles prediction of a two dimensional electron gas at the BiFeO₃/SrTiO₃ interface. *Appl Phys Lett*. 2011;99:423.
40. Yin B, Aguado-Puente P, Qu S, Artacho E. Two-dimensional electron gas at the PbTiO₃/SrTiO₃ interface: An ab initio study. *Phys Rev B*. 2015;92:115406.
41. Aguado-Puente P, Bristowe NC, Yin B, et al. Model of two-dimensional electron gas formation at ferroelectric interfaces. *Phys Rev B*. 2015;92:035438.
42. Cheema SS, Kwon D, Shanker N, Reis RD, Salahuddin S. Enhanced ferroelectricity in ultrathin films grown directly on silicon. *Nature*. 2020;580:478-482.
43. Sang X, Grimley ED, Schenk T, Schroeder U, Lebeau JM. On the structural origins of ferroelectricity in HfO₂ thin films. *Appl Phys Lett*. 2015;106:114113.
44. Xu X, Huang F-T, Qi Y, et al. Kinetically stabilized ferroelectricity in bulk single-crystalline HfO₂:Y. *Nat Mater*. 2021;20:826-832.
45. Huan TD, Sharma V, Rossetti GA, Ramprasad R. Pathways Towards Ferroelectricity in Hafnia. *Phys Rev B*. 2014;90:064111.
46. Wei Y, Nukala P, Salverda M, et al. A rhombohedral ferroelectric phase in epitaxially strained Hf_{0.5}Zr_{0.5}O₂ thin films. *Nat Mater*. 2018;17:1095-1100.
47. Clark SJ, Segall MD, Pickard CJ, et al. First principles methods using CASTEP. *Z Kristallogr Cryst Mater*. 2005;220:567-570.
48. Perdew JP, Burke K, Ernzerhof M. Generalized Gradient Approximation Made Simple. *Phys Rev Lett*. 1998;77:3865-3868.
49. Tagantsev AK, Gerra G. Interface-induced phenomena in polarization response of ferroelectric thin films. *J Appl Phys*. 2006;100:2623-314.
50. Bernardini F, Fiorentini V. Polarization fields in nitride nanostructures: ten points to think about. *Appl Surf Sci*. 2000;166:23-29.
51. Gerra G, Tagantsev AK, Setter N, Parlinski K. Ionic polarizability of conductive metal oxides and critical thickness for ferroelectricity in BaTiO₃. *Phys Rev Lett*. 2006;96:107603.
52. Grimley ED, Schenk T, Sang X, et al. Structural Changes Underlying Field-Cycling Phenomena in Ferroelectric HfO₂ Thin Films. *Adv Electron Mater*. 2016;2:
53. Pešić M, Fengler FPG, Larcher L, et al. Physical Mechanisms behind the Field-Cycling Behavior of HfO₂-Based Ferroelectric Capacitors. *Adv Funct Mater*. 2016;26:4601-4612.
54. Chae K, Kummel AC, Cho K. Hafnium-Zirconium Oxide Interface Models with Semiconductor and Metal for Ferroelectric Devices. *Nanoscale Adv*. 2021.
55. Duan C-G, Sabirianov RF, Mei W-N, Jaswal SS, Tsybalyk EY. Interface Effect on Ferroelectricity at the Nanoscale. *Nano Lett*. 2006;6:483-487.
56. Stengel M, Vanderbilt D, Spaldin NA. Enhancement of ferroelectricity at metal-oxide interfaces. *Nat Mater*. 2009;8:392-397.
57. Sepiarsky M, Stachiotti MG, Migoni RL. Interface effects in ferroelectric PbTiO₃ ultrathin films on a paraelectric substrate. *Phys Rev Lett*. 2006;96:137603.
58. Maintz S, Deringer VL, Tchougréeff AL, Dronskowski R. LOBSTER: A tool to extract chemical bonding from plane-wave based DFT. *J Comput Chem*. 2016;37:1030-1035.
59. Feigl FJ, Fowler WB, Yip KL. Oxygen vacancy model for the E₁' center in SiO₂. *Solid State Commun*. 1974;14:225-229.

60. Shluger A. On the nonequivalency of Si-O bonds in silicon dioxide. *J Phys Chem Solids*. 1986;47:659-664.
61. Xu B, Cooper VR, Singh DJ, Feng YP. Relationship between bond stiffness and electrical energy storage capacity in oxides: Density functional calculations for h-La₂O₃, MgO, and BeO. *Phys Rev B*. 2011;83:064115.
62. Haeni JH, Irvin P, Chang W, et al. Room-temperature ferroelectricity in strained SrTiO₃. *Nature*. 2004;430:758-761.
63. Warusawithana MP, Cen C, Sleasman CR, Woicik JC, Schlom DG. A Ferroelectric Oxide Made Directly on Silicon. *Science*. 2009;324:367-370.
64. Kolpak AM, Walker FJ, Reiner JW, et al. Interface-Induced Polarization and Inhibition of Ferroelectricity in Epitaxial SrTiO₃/Si. *Phys Rev Lett*. 2010;105:217601.